metals

MDPI

Article

Simultaneous Removal of Hg(II) and Phenol Using Functionalized Activated Carbon Derived from *Areca* Nut Waste

Lalhmunsiama [1], Seung Mok Lee [1], Suk Soon Choi [2] and Diwakar Tiwari [3,*]

[1] Department of Environmental Engineering, Catholic Kwandong University, 522 Naegok-dong, Gangneung 210-701, Korea; lhsiama27@gmail.com (L.); leesm@cku.ac.kr (S.M.L.)
[2] Department of Biological and Environmental Engineering, Semyung University, Jecheon 27136, Korea; sschoi@semyung.ac.kr
[3] Department of Chemistry, School of Physical Sciences, Mizoram University, Aizawl 796004, India
* Correspondence: diw_tiwari@mzu.edu.in; Tel.: +91-389-2301806; Fax: +91-389-2330834

Received: 30 April 2017; Accepted: 28 June 2017; Published: 3 July 2017

Abstract: *Areca* nut waste was utilized to obtain high surface area activated carbon (AC), and it was further functionalized with succinic anhydride under microwave irradiation. The surface morphology and surface functional groups of the materials were discussed with the help of scanning electron microscope(SEM) images and fourier transform infra-red (FT-IR) analysis. The specific surface area of the AC and functionalized-AC was obtained by the Brunauer-Emmett-Teller (BET) method, and found to be 367.303 and 308.032 m^2/g, respectively. Batch experiments showed that higher pH favoured the removal of Hg(II), whereas the phenol removal was slightly affected by the changes in the solution pH. The kinetic data followed pseudo-first order kinetic model, and intra-particle diffusion played a significant role in the removal of both pollutants. The maximum sorption capacity of Hg(II) and phenol were evaluated using Langmuir adsorption isotherms, and found to be 11.23 and 5.37 mg/g, respectively. The removal of Hg(II) was significantly suppressed in the presence of chloride ions due to the formation of a $HgCl_2$ species. The phenol was specifically adsorbed, forming the donor–acceptor complexes or π–π electron interactions at the surface of the solid. Further, a fixed-bed column study was conducted for both Hg(II) and phenol. The loading capacity of the column was estimated using the nonlinear Thomas equation, and found to be 2.49 and 2.70 mg/g, respectively. Therefore, the study showed that functionalized AC obtained from *areca* nut waste could be employed as a sustainable adsorbent for the simultaneous removal of Hg(II) and phenol from polluted water.

Keywords: *areca* nut waste; activated carbon; Hg(II); phenol; adsorption

1. Introduction

Water pollution is a serious environmental concern, and is growing rapidly due to the extreme use of harmful substances/chemicals by various industries. The wastewaters produced from manufacturing processes and petroleum refineries usually contain heavy metals and other toxic organic pollutants [1,2]. The partly treated or untreated effluents from these industries greatly contaminate the receiving water bodies. Heavy metals and phenolic compounds, which are the most common water pollutants, are found to be highly toxic towards living organisms and are difficult to eliminate from water bodies or even from the biosystem once entered [3–5]. Mercury has received greater environmental concern due to its high toxicity, persistence in the environment, and high bioaccumulation [6,7]. Dissolved Hg(II) in an aquatic environment is readily transformed into methylmercury, which is a highly toxic, persistent, and bioaccumulative form of mercury present in

nature. Mercury species are volatile, and the inhalation of its vapour produces detrimental effects to the nervous, digestive, and immune systems [8]. Moreover, the intake of mercury was reported to affect the normal growth of the central nervous system, and also causes DNA damage through multiple mechanisms [9]. On the other hand, phenol and its derivatives are potential water pollutants, and have shown adverse effects towards living organisms [10]. Exposure to phenol is reported to be related to protein degeneration, malfunction in the central nervous system, and is able to disturb the function of the kidney, liver, and pancreas in the human body [11]. Furthermore, the phenol present in aquatic environment is easily transformed through a simple oxidation process into chlorophenol, a carcinogenic compound [12]. Therefore, mercury and phenol are classified as priority contaminants, and their acceptable concentration in drinking water according to the United States Environmental Protection Agency (USEPA) is 2 μg/L and 0.5 mg/L, respectively [12,13].

An adsorption technique is largely employed for the removal of a wide range of water pollutants, as it offers several advantages over the conventional methods. The advantages of an adsorption process include high removal efficiency even at a low concentration of pollutants, easy operation and maintenance, flexibility, and the possibility of recovering the material [14]. Activated carbons (ACs) have been extensively used in the removal of mercuric ions from aqueous solutions [15,16]. Moreover, different types of materials, such as electrospun sulfur copolymers [17], lignocellulosic material derived from the Spanish broom plant [18], and lignin [19] were reported as effective adsorbents for reducing Hg(II) concentrations in aquatic media. Recently, Li and co-workers [20] synthesized a mercury "nano-trap" by functionalizing a high surface area porous organic polymer with a high density of strong mercury chelating groups. This mercury "nano-trap" exhibits an extremely high uptake capacity of mercury, i.e., over 1000 mg/g and can effectively reduce Hg(II) concentration to acceptable limits of drinking water standards . ACs and their modified materials were also efficiently utilized for the treatment of aqueous effluents polluted with phenol [21–23]. AC is undoubtedly one of the most effective materials in wastewater treatment due to its large specific surface area, porous structure, and high performance. In spite of possessing high sorption capacity, the use of commercial AC is not viable because of its high cost. Therefore, many researchers have utilized waste materials, such as rice husk, sugarcane bagasse [24], grape bagasse [25], peanut shell [26], and coconut husk [27], for obtaining low cost ACs to employ in the removal of various pollutants from an aquatic environment.

Areca nut, popularly known as betel nut, is widely cultivated in many Asian countries and parts of Africa. *Areca* nut waste, a lignocellulose material, is available in large quantities in many countries and there is no report about its possible application for useful purposes [28]. The conversion of *areca* nut waste into AC could probably be an alternative method to exploit this agriculture by-product in bioremediation [29]. Previously, the AC prepared from *areca* nut waste was utilized in the removal of hexavalent chromium [30,31], congo red [32], direct blue [33], and acid blue [34] from aqueous solutions. Therefore, the present work aims to utilize this abundantly available agriculture by-product for the preparation of AC and its further functionalization with succinic anhydride under microwave irradiation. The incorporation of succinic anhydride possibly increases the number of active functional groups onto the AC's surface, and subsequently enhances the interaction of the materials with pollutants. Previously, agriculture waste materials such as maize straw [35], olive stone [36], corncob [37], and sugarcane bagasse [38] were modified with succinic anhydride, and the materials were found to be efficient in the removal of several toxic metal ions from aqueous solutions. In this study, AC was prepared from *areca* nut waste and it was further functionalized using succinic anhydride under microwave irradiation. The microwave-assisted method employed for the functionalization of AC offers several advantages over the conventional methods in terms of selectivity in operation, fast and uniform irradiation, and reducing reaction time and energy. Furthermore, there is no report on the simultaneous removal of organic and inorganic pollutants using succinic anhydride functionalized activated carbons, so it is interesting to assess these materials for the simultaneous removal of toxic heavy metals and organic contaminants from aqueous media. Therefore, the functionalized-AC was

assessed for its capability to remove Hg(II) and phenol simultaneously from aqueous solutions under batch and fixed-bed adsorption systems.

2. Materials and Methods

2.1. Materials

The *areca* nut waste was collected from Aizawl city, Mizoram, India. It was repeatedly washed with pure water to remove any impurity, and then dried in an oven (Chang Shin Scientific Co., Busan, South Korea) (at 80 °C. Dry *areca* nut waste was soaked in concentrated H_2SO_4 for 2 h at the temperature of 120 °C. The solid biomass was then completely transformed into its carbon form. The obtained carbon was carefully washed with pure water to eliminate excess acids, and dried at 70 °C. Any excess acid remaining within the carbon solid was then titrated with ammonia solution for neutralization. The carbon was again washed with distilled water several times until the pH reached ~7.0, and then finally dried at 70 °C. The solid sample was cooled and then ground to obtain fine powder. Furthermore, the carbon powder was activated in a muffle furnace (Chang Shin Scientific Co., Busan, South Korea) at 500 °C for 4 h under an N_2 atmosphere. The activated carbon obtained was then kept inside a close plastic container for further use.

2.2. Modification of Activated Carbon

The functionalization of the activated carbon was carried out as follows: 5.0 g of succinic anhydride was dissolved in 100 mL of acetone. Ten grams (10 g) of activated carbon obtained from *areca* nut waste was added to this succinic anhydride solution. The mixture was kept under microwave irradiation at 60 °C for 60 min with constant stirring (Model: MAS II, Sineo Microwave Chemistry Technology Co., Ltd., Shanghai, China). The functionalized activated carbon was separated and washed with distilled water three times and then dried completely at 80 °C. The functionalized-AC was used for the simultaneous removal of Hg(II) and phenol under batch and fixed-bed column systems.

2.3. Characterization of Materials

The surface morphology of the AC before and after functionalization was observed by the SEM (scanning electron microscope) analysis (FE-SEM-Model: SU-70, Hitachi, Tokyo, Japan). The specific surface area of the activated carbon before and after functionalization was measured by the Brunauer-Emmett-Teller (BET) surface area analyzer (Model: ASAP 2020, Protech Korea Co. Ltd, Seoul, South Korea). Moreover, Fourier Transform Infra-Red (FT-IR) spectroscopy (Tensor 27, Bruker Co., Billerica, MA, USA) was used for the identification of various functional groups present in the AC and functionalized-AC solids.

2.4. Batch Adsorption Experiment

Batch experiments were performed to study the effect of pH, initial Hg(II)/phenol concentrations, contact time, and background electrolyte concentrations on the removal of Hg(II) and phenol using functionalized-AC. The experiments were performed using 0.10 g of functionalized-AC taken into 50 mL of Hg(II)/phenol solution and kept in an automatic shaker (Kukje Machinery Co., Ltd., Okcheon, South Korea) for 12 h at 25 °C. The solution was filtered using a 0.45 μm syringe filter, and the final concentration of Hg(II) was analyzed by a fast sequential atomic absorption spectrometer (AAS) (Model: AA240FS, Varian, Australia), whereas the phenol concentration was measured using a UV-visible spectrophotometer (Model: Humas HS 3300, Humas Co., Ltd., Daejeon, South Korea). The pH of the solutions was adjusted by adding drops of 1 M HCl or 1 M NaOH.

2.5. Fixed-Bed Column Adsorption

A glass column with a 1 cm inner diameter was used for performing a fixed-bed column experiments. Accurately 1.0 g of functionalized-AC was firmly packed in the middle of the column

using glass beads. The aqueous solution containing both Hg(II) and phenol was pumped upward by a high-pressure liquid chromatographic pump (Acuflow Series II, Dongwoo Science Co., Ltd., Hanam, South Korea), and the flow rate was maintained at 0.5 mL/min. The effluent samples were collected using a Spectra/Chrom CF-2 fraction collector (Model: Retriever 500, Teledyne ISCO, Lincoln, NE, USA), and then filtered with a 0.45 μm syringe filter. The concentration of Hg(II) and phenol in the effluent was measured using an AAS and a UV-vis spectrophotometer, respectively.

3. Results and Discussion

3.1. Characterization of Materials

The SEM micrographs of the *areca* nut waste AC and functionalized-AC are shown in Figure 1. The macropores present in the AC solids are clearly visible, and the pore diameters are found to be in the range of 5–15 μm as obtained from the SEM images. Further, the smaller pores were also visible in the SEM image of the AC. Figure 1b shows an SEM image of the functionalized-AC. It is observed that the incorporation of succinic anhydride significantly changed the surface morphology of the AC, and the pores are less visible after the functionalization of the AC. A previous report also had shown that the surface morphology of maize straw was significantly changed after the incorporation of succinic anhydride [35]. The nitrogen adsorption isotherms of the AC and functionalized-AC are shown in Figure 2. According to International Union of Pure and Applied Chemistry (IUPAC) classification, the two solid samples display a H4 type hysteresis loop [39]. The specific surface area of the AC was found to be 367.30 m^2/g. The surface area slightly decreased to 308.03 m^2/g after the incorporation of succinic anhydride. This decrease in specific surface area is ascribed due to the accumulation of succinic anhydride within the pores of the AC. Moreover, the incorporation of succinic anhydride within the pores of AC caused a slight decrease in the pore size and pore volume of the AC, from 3.13 to 2.78 nm and from 0.028 to 0.016 cm^3/g, respectively.

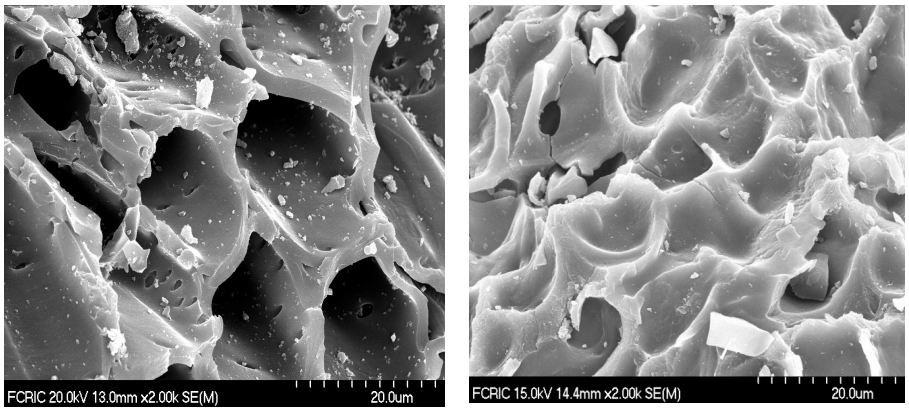

(**a**) (**b**)

Figure 1. Scanning electron microscope (SEM) micrograph of (**a**) activated carbon (AC) and (**b**) functionalized-AC.

The FT-IR analytical results are graphically shown in Figure 3. The predominant peak that appeared at around 3434 cm^{-1} is attributed to the stretching vibration of –OH groups. Several weak peaks obtained at 2856, 2925, and 2972 cm^{-1} are attributed to the presence of aldehyde groups and assigned to the stretching and scissoring of C–H bonds. Moreover, the bands that occurred at 1620 and 1700 cm^{-1} are assigned to the C=C and C=O groups [40]. Further, the vibration peaks in the region of 1042 cm^{-1} are due to the C–O–C stretching [36]. The weak peaks that occurred at around 1458 cm^{-1} showed the C–H vibration in $–CH_2–$ deformation. Moreover, other vibration bands that occurred at 874 and 740 cm^{-1} are due to an external bending of –C–H for various substituted benzene rings [41].

It is worth mentioning that the intensity of the peak occurred at 1700 cm^{-1} (it appeared as a shoulder), which indicates that the stretching vibration of the C=O group is significantly increased after the functionalization of AC. These changes eventually indicate the successful incorporation of succinic anhydride into the AC solids [42]. Previous studies have shown that a new distinguished peak was observed at around 1730 cm^{-1} after the incorporation of succinic anhydride into *posidonia* and maize straw [35,43]. However, in this study, a new peak overlapped with the pre-existing peaks and caused an increase in the peak intensity. Furthermore, the decrease in the intensities of the absorption band at 1042 cm^{-1} assigned for the C–O–C bond stretching suggests the succinylation of the AC [35,36].

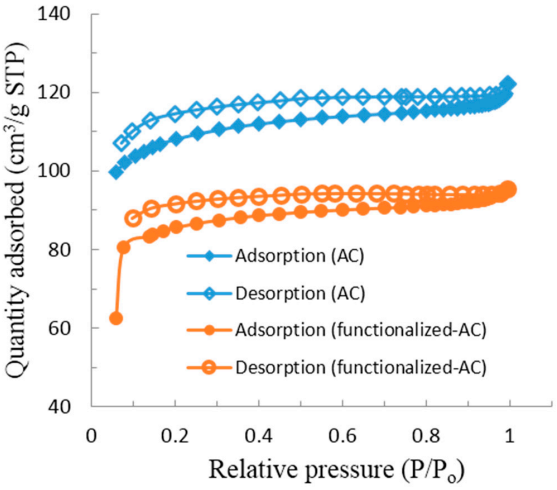

Figure 2. Nitrogen adsorption–desorption isotherm of AC and functionalized-AC.

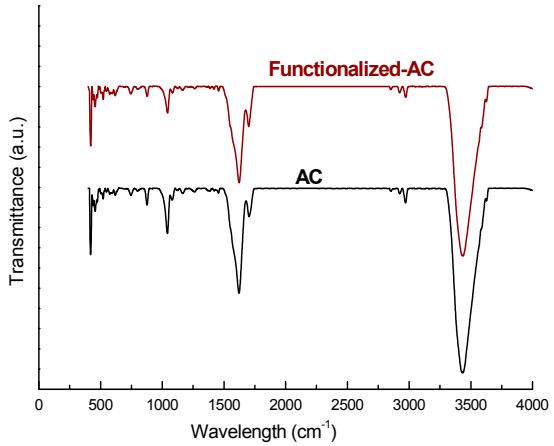

Figure 3. Fourier transform infra-red (FT-IR) spectra obtained for AC and functionalized-AC.

3.2. Batch Adsorption Experiments

3.2.1. Effect of pH on Hg(II)/Phenol Adsorption

pH is a crucial parameter influencing the adsorption of Hg(II) and phenol from aqueous solutions, since it determines the speciation of Hg(II) and/or the ionization of phenol as well as the surface charge of the adsorbents [44,45]. Therefore, the effect of pH was studied between pH 2.0 and 8.0 using a solution containing 5.4 mg/L of Hg(II) and 9.36 mg/L of phenol. The percentage removal of Hg(II) and phenol as a function of initial pH is shown in Figure 4. The pH dependence study showed that Hg(II) removal was significantly increased while increasing the solution pH from 2.0 to 4.0, and remained almost unchanged beyond pH 4.0. At low pH, the percentage sorption of Hg(II) was

relatively low, due to the competition between Hg^{2+} and H^+ ions towards the same active sites on the functionalized-AC [38]. At higher pH values, the H^+ ions concentration is decreased, and consequently enhances the uptake of Hg(II) ions from aqueous solutions. A previous report also showed that Hg(II) removal using activated biocarbon was relatively low at lower pH values and increased under higher pH conditions [46]. Conversely, phenol removal was slightly affected by changing the solution pH from 2.0 to 8.0. It was reported that phenol predominantly existed in its undissociated form within the pH region between 2.0 and 8.0; therefore, the adsorption of phenol was insignificantly influenced by the solution pH [3]. A similar trend was previously observed in the removal of phenol as a function of pH using activated carbon fibers and surface functionalized activated sericite [47,48].

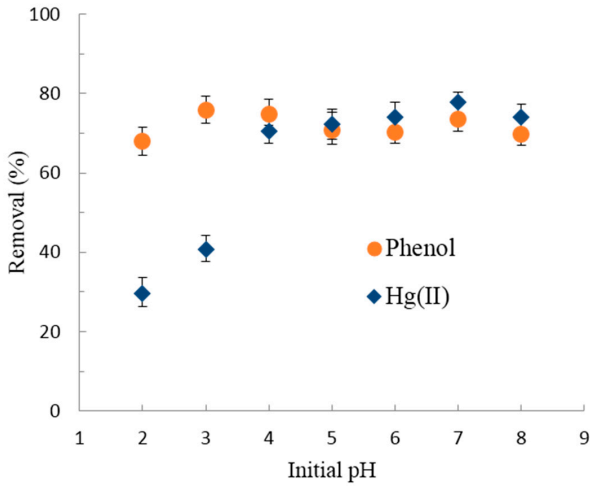

Figure 4. Effect of pH in the removal of Hg(II) and Phenol by functionalized-AC from aqueous solutions (Initial (Hg(II)/phenol) concentration: ~10 mg/L, solid dose: 2.0 g/L, contact time: 12 h).

3.2.2. Adsorption Kinetics of Hg(II) and Phenol

In order to obtain the adsorption equilibrium time of Hg(II) and phenol by functionalized-AC, the extent of the removal at various intervals of time was analyzed, while keeping a constant solution pH, and the initial concentration of Hg(II) and phenol at ~10 mg/L. The percentage removal of Hg(II)/phenol at various intervals of time is given in Figure 5. The two pollutants exhibit similar sorption kinetics, which arerelatively slow. The percentage adsorption of Hg(II) and phenol continuously increases, and adsorption equilibrium is achieved within 300 min of contact time for both Hg(II) and phenol.

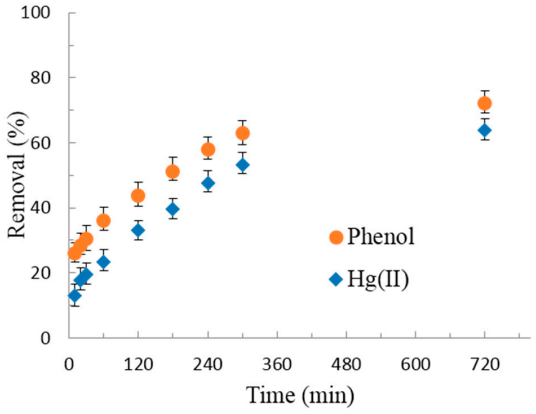

Figure 5. Percentage removal of Hg(II) and phenol using functionalized-AC at various intervals of time (Initial (Hg(II)/phenol) concentrations: ~10 mg/L, pH: 5.0, solid dose: 2.0 g/L, contact time: 12 h).

The pseudo-first order kinetic (Equation (1)) and pseudo-second order kinetic (Equation (2)) models were employed to perform the kinetic modelling using the time dependent adsorption data of Hg(II) and phenol by the functionalized-AC. The equations were taken in their linear form:

$$\ln(q_e - q_t) = \ln q_e - k_1 t \quad (1)$$

$$\frac{t}{q_t} = \frac{1}{k_2 q_e^2} + \frac{t}{q_e} \quad (2)$$

where q_e is the maximum amount of Hg(II)/phenol adsorbed at equilibrium (mg/g), and q_t (mg/g) is the amount of the Hg(II) or phenol adsorbed at time t. k_1 (min^{-1}) and k_2 (g/mg/min) are the adsorption rate constants of the pseudo-first order and the pseudo-second order models, respectively [49]. The unknown values such as q_e, k_1, and k_2 were calculated from a plot of $\ln(q_e - q_t)$ versus t, and the plots of $\frac{t}{q_t}$ against t, respectively, for the pseudo-first order kinetic and pseudo-second order kinetic models, and returned in Table 1. The R^2 values indicated that the adsorption kinetic data fitted well to the pseudo-second order kinetic model rather than the pseudo-first order kinetic model for both the pollutants.

In porous materials, intra-particle diffusion usually plays a crucial role in controlling the adsorption of various pollutants from aqueous solutions. Therefore, the time-dependent intra-particle diffusion rate of Hg(II)/phenol from the outer surface active sites to the inside pores of the functionalized-AC was evaluated using an intra-particle diffusion model (Equation (3)) developed by Weber and Morris [50]. The equation is taken as:

$$q_t = k_{id} t^{\frac{1}{2}} + Z \quad (3)$$

where k_{id} is the intra-particle diffusion rate constant (g/mg/$min^{1/2}$), and Z is the intercept. The graph was plotted for the amount of Hg(II)/phenol adsorbed at various contact times (q_t) against the square root of time ($t^{1/2}$) and illustrated in Figure 6. The intra-particle diffusion plots for Hg(II) and phenol showed a good linearity with a high R^2 values, which indicated that intra-particle diffusion contributed a vital role in the sorption of Hg(II) and phenol onto functionalized-AC. However, a minor divergence from the origin was observed in the case of phenol, which was perhaps due to the variation in the solutes movement during the initial and final steps of the adsorption process [51]. The intra-particle diffusion constants along with the R^2 values are summarized in Table 1.

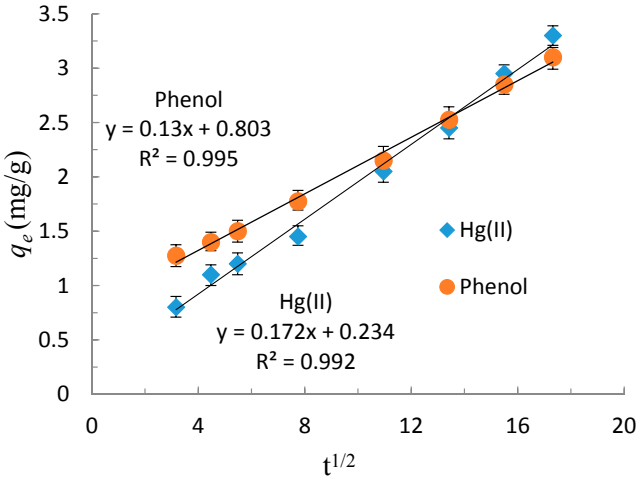

Figure 6. Plots of the intra-particle diffusion model for Hg(II) and phenol removal using functionalized-AC (Initial (Hg(II)/phenol) concentrations: ~10 mg/L, pH: 5.0, solid dose: 2.0 g/L, contact time: 12 h).

Table 1. Rate constants (k_1 and k_2), sorption capacity (q_e), and R^2 values obtained from the pseudo-first order and pseudo-second order kinetic models, along with the intra-particle diffusion constants obtained for the adsorption of Hg(II) and phenol by functionalized-AC.

Sample	Pseudo-First Order Kinetic			Pseudo-Second Order Kinetic			Intra-Particle Diffusion		
	k_1 (1/min)	q_e (mg/g)	R^2	k_2 (g/mg/min)	q_e (mg/g)	R^2	K_{id} (mg/g/min$^{1/2}$)	Z	R^2
Hg(II)	5.0×10^{-3}	1.72	0.95	1.0×10^{-2}	3.19	0.97	0.12	0.23	0.99
Phenol	5.0×10^{-3}	1.48	0.90	6.0×10^{-3}	3.27	0.95	0.13	0.80	0.99

3.2.3. Adsorption Isotherm Studies

The effect of initial Hg(II) concentration was studied, increasing the initial concentration from 2.0 to 25.0 mg/L in the presence of 10.0 mg/L phenol at pH 5.0. Similarly, the effect of initial phenol concentration was studied, increasing the initial concentration from 1.0 to 20.0 mg/L in presence of 10.0 mg/L Hg(II) at pH 5.0. The equilibrium stage sorption data obtained were plotted between the percentage removals against the initial bulk sorptive concentrations (mg/L) and graphically shown in Figure 7a,b. An enhanced percentage of adsorption was observed at lower concentration of solutes, especially in the case of phenol, and gradually reduced with increasing the initial sorptive concentration. The uptake amount of Hg(II) and phenol was found to be increased from 0.65 to 5.65 mg/g and 0.58 and 5.44 mg/g, respectively, while increasing the initial sorptive concentrations as mentioned above. It is interesting to observe that the percentage removal of phenol remained almost unchanged while increasing the initial concentration of Hg(II) from 2.0 to 25.0 mg/L (Figure 7a). Similarly, there was no significant effect on Hg(II) removal by increasing the phenol concentration from 1.0 to 20 mg/L (Figure 7a). Therefore, these studies infer that the functionalized-AC is able to remove Hg(II) and phenol simultaneously from water, and suggest the presence of different binding sites available for these two different types of pollutants [48].

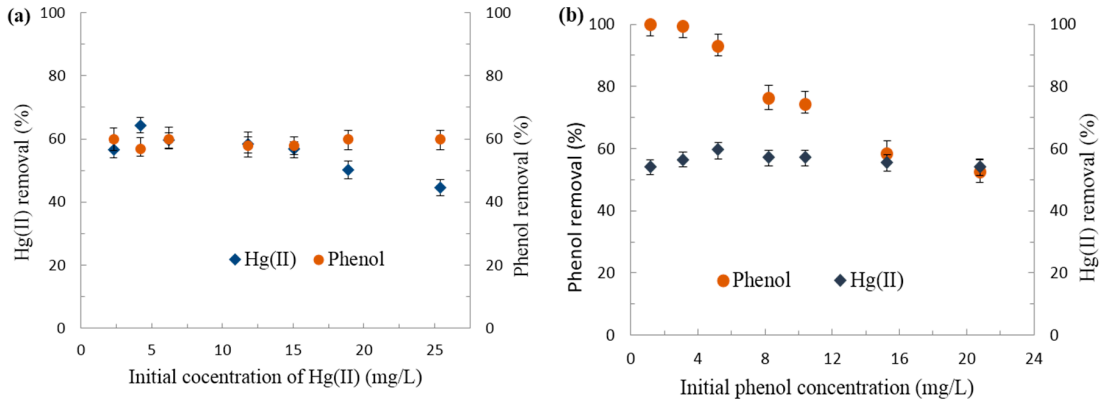

Figure 7. The concentration dependence removal of (**a**) Hg(II) in presence of ~10 mg/L phenol (Initial (Hg(II)) concentration: 1–25 mg/L, pH: 5.0, solid dose: 2.0 g/L, contact time: 12 h) and (**b**) phenol in presence of ~10 mg/L Hg(II) (Initial (phenol) concentration: 1–20 mg/L, pH: 5.0, solid dose: 2.0 g/L, contact time: 12 h).

The equilibrium state adsorption data obtained at various sorptive concentrations were further modeled using Langmuir (Equation (4)) and Freundlich (Equation (5)) adsorption isotherms. The adsorption models were taken to its nonlinear forms [52]:

$$q_e = \frac{q_m K_L C_e}{1 + K_L C_e} \tag{4}$$

$$q_e = K_F C_e^{\frac{1}{n}} \tag{5}$$

where q_e is the amount of Hg(II)/phenol adsorbed (mg/g) by functionalized-AC, and C_e is the bulk Hg(II)/phenol concentration (mg/L) at equilibrium. K_L is the Langmuir rate constant (L/g), and q_m is the Langmuir monolayer sorption capacity (mg/g). K_F is the Freundlich constant, which corresponds to the adsorption capacity (mg/g), and $1/n$ is the sorption intensity. The nonlinear plot of the Langmuir and Freundlich adsorption isotherms for the removal of Hg(II) and phenol are shown in Figure 8a,b, respectively. Moreover, the adsorption capacity of functionalized-AC for Hg(II) and phenol along with the isotherm constants values are given in Table 2. The adsorption of Hg(II) onto functionalized-AC at various concentrations followed the Freundlich isotherm rather than the Langmuir model, whereas the experimental data obtained for phenol adsorption on functionalized-AC were reasonably fitted well to both the Langmuir and Freundlich models. Furthermore, the adsorption isotherm studies were conducted for the bare activated carbon under the identical experimental conditions. Langmuir and Freundlich adsorption isotherm studies were conducted for the adsorption of Hg(II) and phenol by the activated carbon obtained from *areca* nut waste, and the results are shown in Figure 8a,b. The isotherm constants values are summarized in Table 2. It is observed that the Langmuir monolayer adsorption capacity for Hg(II) was doubled after the functionalization with succinic anhydride. Moreover, the functionalization of the AC caused an increase in the adsorption capacity of phenol from 3.846 to 5.555 mg/g.

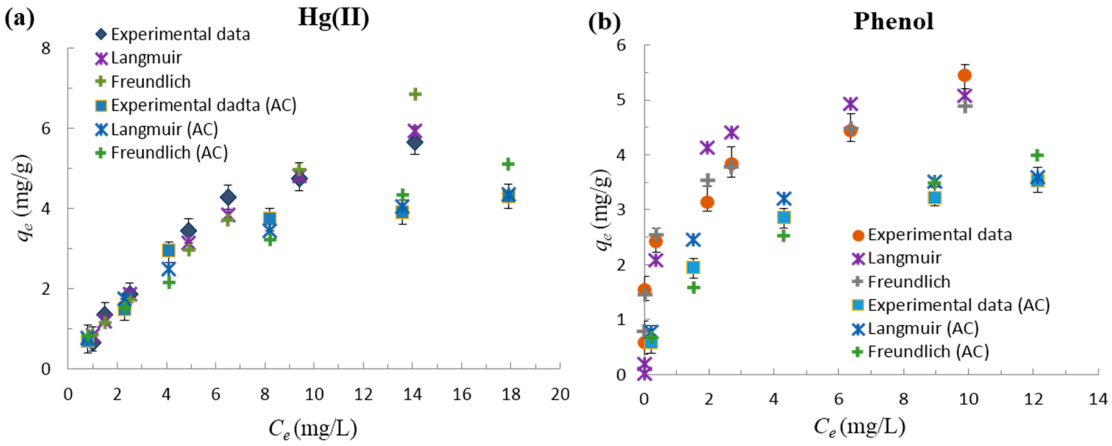

Figure 8. Plots of Langmuir and Freundlich adsorption isotherms for the removal of (**a**) Hg(II) and (**b**) phenol using functionalized-AC and bare AC.

Table 2. Langmuir and Freundlich constants along with R^2 values obtained for the removal of Hg(II) and phenol using modified-AC.

Material	Pollutant	Langmuir			Freundlich		
		q_o (mg/g)	K_L (L/g)	R^2	1/n	K_F(mg/g)	R^2
Functionalized-AC	Hg(II)	11.235	0.079	0.848	0.792	0.843	0.953
Activated carbon (AC)	Hg(II)	5.555	0.199	0.977	0.586	0.942	0.925
Functionalized-AC	Phenol	5.376	1.706	0.970	0.198	3.104	0.968
AC	Phenol	3.846	0.116	0.997	0.443	1.320	0.954

3.2.4. Effect of Background Electrolyte Concentrations

The effect of background electrolyte concentrations is a significant parameter to study the binding nature of pollutants onto the solid materials, and it is usually exploited to make a distinction between non-specific and specific adsorption. Specific sorption is unaffected by varying the background electrolyte concentration, whereas non-specific adsorption is significantly affected by increasing the background electrolyte concentrations [53,54]. In order to study the adsorption nature of Hg(II) and phenol onto functionalized-AC, an effect of background electrolyte concentration study was conducted, using NaCl as a background electrolyte. Similarly, the removal behaviour of Hg(II) was studied in

the presence of $NaNO_3$. The concentration of Hg(II) and phenol was maintained at approximately 5 mg/L at pH 5.0, and the concentration of NaCl and $NaNO_3$ was increased from 0.001 to 0.1 mol/L. The percentage removal of mercury and phenol as a function of background electrolytes is shown in Figure 9. It was observed that an increase in NaCl concentrations from 0.001 to 0.1 mol/L caused a considerable decrease in the uptake of Hg, while an increase in the concentration of $NaNO_3$ to the same extent did not affect the Hg(II) removal. A large decrease in mercury removal in the presence of NaCl was explained with the help of mercury speciation. In aqueous solution, Hg(II) forms various complexes with the chlorides, i.e., $HgCl^+$, $HgCl_2$, $HgCl_3^-$, and $HgCl_4^{2-}$, along with the mixed species Hg(OH)Cl. In the pH region between 3.5 and 5.5, the $HgCl_2$ is a predominant species (i.e., over 80%) [18,19]. Meanwhile, the adsorption experiment was carried out at pH 5.0 in the presence of chloride, in which the predominant species is $HgCl_2$. Therefore, the $HgCl_2$ species were not efficiently removed by the functionalized-AC, and caused a drastic decrease in the removal of mercury from the aqueous solutions. Alternatively, the uptake of Hg(II) remained almost constant while increasing the $NaNO_3$ concentrations from 0.001 to 0.1 mol/L. These results suggested that the Hg(II) ions were specifically adsorbed and formed 'inner sphere complexes' on the surface of functionalized-AC [53]. On the other hand, the percentage removal of phenol was remained constant while increasing the NaCl concentration from 0.001 to 0.1 mol/L. This result suggested that phenols were also specifically adsorbed through the formation of donor–acceptor complexes, in which the carbonyl group of the functionalized-AC is an electron donor and the aromatic rings of phenol are electron acceptors [55]. Moreover, phenols were trapped within the pores of the solid materials, and possibly forming a strong bond through the π–π electron interaction of the benzene ring in phenol and π-electrons present with the solid materials [56,57].

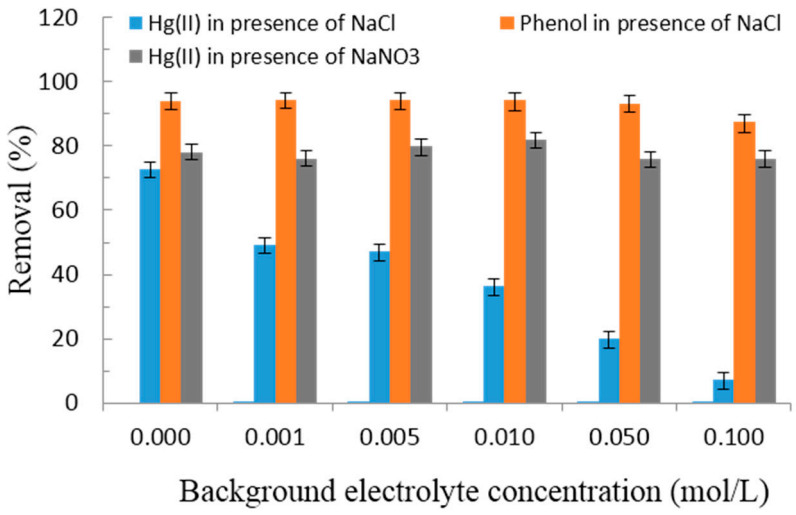

Figure 9. Effect of background electrolyte concentrations in the removal of Hg(II) and phenol by modified-AC from aqueous solutions (Initial (Hg(II)/phenol) concentrations: ~10 mg/L, pH: 5.0, solid dose: 2.0 g/L, contact time: 12 h, background electrolyte: $NaCl/NaNO_3$).

3.3. Fixed-Bed Column Adsorption

In addition to batch reactor experiments, a fixed-bed column adsorption study was conducted. In this study, the pH of the influent solution was maintained at pH 5.0, and the initial concentrations of Hg(II) and phenol was taken 4.5 and 7.89 mg/L, respectively. It was observed that the functionalized-AC could efficiently remove the Hg(II) and phenol even in a continuous flow system. The nonlinear Thomas equation (Equation (6)) was utilized to fit breakthrough data obtained for Hg(II)

and phenol to optimize the loading capacity of functionalized-AC under dynamic conditions [58]. The equation is taken as:

$$\frac{C_e}{C_o} = \frac{1}{1 + e^{(K_T(q_o m - C_o V))/Q}} \quad (6)$$

where C_e is the concentration of Hg(II)/phenol in the effluent (mg/L); C_o is the initial concentration of Hg(II)/phenol in the feed solution (mg/L); K_T is the Thomas rate constant (L/min/mg); q_o is the loading capacity of Hg(II)/phenol (mg/g); m is the mass of functionalized-AC packed inside the column (g); V is the volume of water passed through the column (L); and Q is the influent flow rate (L/min). As shown in Figure 10, the column data were reasonably fitted well to the nonlinear Thomas equation, and the loading capacities (q_o) of Hg(II) and phenol were found to be 2.49 and 2.70 mg/g, respectively. Moreover, the Thomas rate constants (K_T) were calculated as 2.13×10^{-3} and 1.09×10^{-3} L/min/mg for Hg(II) and phenol, respectively. The loading capacities obtained from the fixed-bed column adsorption were comparatively lower than that obtained from the batch reactor studies. This is perhaps due to insufficient contact time provided for the solutes Hg(II)/phenol towards the functionalized-AC solid inside the column [59].

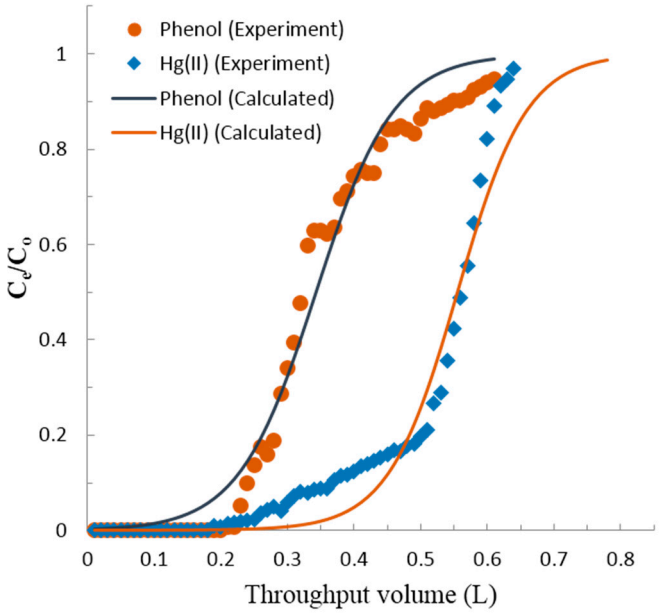

Figure 10. Breakthrough curve of Hg(II) and phenol (pH: 5.0; Initial (Hg(II)) concentration: 4.5 mg/L, Initial (phenol) concentration: 7.89 mg/L; Flow rate: 0.5 mL/min).

4. Conclusions

The succinic anhydride was successfully incorporated with the activated carbon obtained from *areca* nut wastes. The functionalized-AC was employed for the simultaneous removal of Hg(II) and phenol from aqueous solutions. The materials were characterized by the SEM, FT-IR, and BET analyses. The batch adsorption experiment showed that increasing the solution pH favored Hg(II) removal whereas phenol removal was not significantly affected by the variation of the solution pH. The kinetic studies showed that an apparent sorption equilibrium was achieved within 300 min of contact, and it was further observed that intra-particle diffusion contributed a significant role in the removal of Hg(II) and phenol. The equilibrium state sorption data for Hg(II) were well simulated with the Freundlich adsorption isotherm, whereas the sorption data obtained for phenol were reasonably fitted to both the Langmuir and Freundlich models. The maximum sorption capacity was evaluated using Langmuir adsorption isotherms and found to be 11.235 and 5.376 mg/g for Hg(II) and phenol, respectively. The removal of Hg(II) was significantly suppressed in the presence of NaCl due to the formation of $HgCl_2$

species. On the other hand, the phenol removal was insignificantly changed with an increase in NaCl concentrations, which indicated that phenols were adsorbed specifically onto the functionalized-AC. Meanwhile, an increase in the concentration of another background electrolyte, i.e., $NaNO_3$, from 0.001 to 0.1 mol/L did not affect the uptake of Hg(II), and it was assumed that the adsorbed Hg(II) formed 'inner sphere complexes' on the surface of the functionalized-AC. Further, the loading capacities of Hg(II) and phenol under dynamic conditions were evaluated using the nonlinear Thomas equation, and were found to be 2.49 and 2.70 mg/g, respectively. Therefore, the present study suggested that the low cost activated carbon obtained from *areca* nut waste and further functionalized with succinic anhydride under microwave irradiation could be effectively employed in the simultaneous removal of Hg(II) and phenol from the wastewater samples.

Acknowledgments: This work was supported by research fund of Catholic Kwandong University (CKURF-201601200001).

Author Contributions: Lalhmunsiama and Seung Mok Lee conceived and designed the experiments; Lalhmunsiama performed the entire experiments. Diwakar Tiwari and Suk Soon Choi analyzed the experimental data. Further, Lalhmunsiama and Diwakar Tiwari wrote and finalized the paper.

Conflicts of Interest: The authors declare no conflict of interest.

References

1. Han, J.; Du, Z.; Zou, W.; Li, H.; Zhang, C. In-situ improved phenol adsorption at ions-enrichment interface of porous adsorbent for simultaneous removal of copper ions and phenol. *Chem. Eng. J.* **2015**, *262*, 571–578. [CrossRef]
2. Shim, J.; Lim, J.-M.; Shea, P.J.; Oh, B.-T. Simultaneous removal of phenol, Cu and Cd from water with corn cob silica-alginate beads. *J. Hazard. Mater.* **2014**, *272*, 129–136. [CrossRef] [PubMed]
3. Cheng, W.P.; Gao, W.; Cui, X.; Ma, J.H.; Li, R.F. Phenol adsorption equilibrium and kinetics on zeolite X/activated carbon composite. *J. Taiwan Inst. Chem. Eng.* **2016**, *62*, 192–198. [CrossRef]
4. Fadzil, F.; Ibrahim, S.; Hanafiah, M.A.K.M. Adsorption of lead(II) onto organic acid modified rubber leaf powder: Batch and column studies. *Process. Saf. Environ. Prot.* **2016**, *100*, 1–8. [CrossRef]
5. Pacyna, E.G.; Pacyna, J.M.; Sundseth, K.; Munthe, J.; Kindbom, K.; Wilson, S.; Steenhuisen, F.; Maxson, P. Global emission of mercury to the atmosphere from anthropogenic sources in 2005 and projections to 2020. *Atmos. Environ.* **2010**, *44*, 2487–2499. [CrossRef]
6. Han, C.; Wang, W.; Xie, F. Study on the leaching of mercuric oxide with thiosulfate solutions. *Metals* **2016**, *6*, 206. [CrossRef]
7. Solis, K.L.; Nam, G.-U.; Hong, Y. Effectiveness of gold nanoparticle-coated silica in the removal of inorganic mercury in aqueous systems: Equilibrium and kinetic studies. *Environ. Eng. Res.* **2016**, *21*, 99–107. [CrossRef]
8. Ferreira, S.L.C.; Lemos, V.A.; Silva, L.O.B.; Queiroz, A.F.S.; Souza, A.S.; Silva, E.G.P.; Santos, W.N.L.; Virgens, C.F. Analytical strategies of sample preparation for the determination of mercury in food matrices—A review. *Microchem. J.* **2015**, *121*, 227–236. [CrossRef]
9. Crespo-López, M.E.; Macêdo, G.L.; Pereira, S.I.D.; Arrifano, G.P.F.; Picanço-Diniz, D.L.W.; Nascimento, J.L.M.; Herculano, A.M. Mercury and human genotoxicity: Critical considerations and possible molecular mechanisms. *Pharmacol. Res.* **2009**, *60*, 212–220. [CrossRef] [PubMed]
10. Singh, J.; Yang, J.-K.; Chang, Y.-Y. Rapid degradation of phenol by ultrasound-dispersed nano-metallic particles (NMPs) in the presence of hydrogen peroxide: A possible mechanism for phenol degradation in water. *J. Environ. Manag.* **2016**, *175*, 60–66. [CrossRef] [PubMed]
11. Păcurariu, C.; Mihoc, G.; Popa, A.; Muntean, S.G.; Ianoş, R. Adsorption of phenol and p-chlorophenol from aqueous solutions on poly (styrene-co-divinylbenzene) functionalized materials. *Chem. Eng. J.* **2013**, *222*, 218–227. [CrossRef]
12. Cheng, Z.; Fu, F.; Pang, Y.; Tang, B.; Lu, J. Removal of phenol by acid-washed zero-valentaluminium in the presence of H_2O_2. *Chem. Eng. J.* **2015**, *260*, 284–290. [CrossRef]
13. Huber, J.; Leopold, K. Nanomaterial-based strategies for enhanced mercury trace analysis in environmental and drinking waters. *TrAC Trends Anal. Chem.* **2016**, *80*, 280–292. [CrossRef]

14. Sadeek, S.A.; Negm, N.A.; Hefni, H.H.H.; Wahab, M.M.A. Metal adsorption by agricultural biosorbents: Adsorption isotherm, kinetic and biosorbents chemical structures. *Int. J. Biol. Macromol.* **2015**, *81*, 400–409. [CrossRef] [PubMed]
15. Hadi, P.; To, M.-H.; Hui, C.-W.; Lin, C.S.K.; McKay, G. Aqueous mercury adsorption by activated carbons. *Water Res.* **2015**, *73*, 37–55. [CrossRef] [PubMed]
16. Zhang, F.-S.; Nriagu, J.O.; Itoh, H. Mercury removal from water using activated carbons derived from organic sewage sludge. *Water Res.* **2005**, *39*, 389–395. [CrossRef] [PubMed]
17. Thielke, M.W.; Bultema, L.A.; Brauer, D.D.; Richter, B.; Fischer, M.; Theato, P. Rapid mercury(II) removal by electrospun sulfur copolymers. *Polymers* **2016**, *8*, 266. [CrossRef]
18. Arias, F.E.A.; Beneduci, A.; Chidichimo, F.; Furia, E.; Straface, S. Study of the adsorption of mercury(II) on lignocellulosic materials under static and dynamic conditions. *Chemosphere* **2017**, *180*, 11–23. [CrossRef] [PubMed]
19. Lv, J.; Luo, L.; Zhang, J.; Christie, P.; Zhang, S. Adsorption of mercury on lignin: Combined surface complexation modeling and X-ray absorption spectroscopy studies. *Environ. Pollut.* **2012**, *162*, 255–261. [CrossRef] [PubMed]
20. Li, B.; Zhang, Y.; Ma, D.; Shi, Z.; Ma, S. Mercury nano-trap for effective and efficient removal of mercury(II) from aqueous solution. *Nat. Commun.* **2014**, *5*, 5537. [CrossRef] [PubMed]
21. Lin, S.-H.; Juang, R.-S. Adsorption of phenol and its derivatives from water using synthetic resins and low-cost natural adsorbents: A review. *J. Environ. Manag.* **2009**, *90*, 1336–1349. [CrossRef] [PubMed]
22. Abussaud, B.; Asmaly, H.A.; Ihsanullah; Saleh, T.A.; Gupta, V.K.; laoui, T.; Atieh, M.A. Sorption of phenol from waters on activated carbon impregnated with iron oxide, aluminum oxide and titanium oxide. *J. Mol. Liq.* **2016**, *213*, 351–359. [CrossRef]
23. Feng, J.; Qiao, K.; Pei, L.; Lv, J.; Xie, S. Using activated carbon prepared from TyphaorientalisPresl to remove phenol from aqueous solutions. *Ecol. Eng.* **2015**, *84*, 209–217. [CrossRef]
24. Dalai, C.; Jha, R.; Desai, V.R. Rice husk and sugarcane baggase based activated carbon for iron and manganese removal. *Aquat. Procedia* **2015**, *4*, 1126–1133. [CrossRef]
25. Demiral, H.; Güngör, C. Adsorption of copper(II) from aqueous solutions on activated carbon prepared from grape bagasse. *J. Clean. Prod.* **2016**, *124*, 103–113. [CrossRef]
26. AL-Othman, Z.A.; Ali, R.; Naushad, M. Hexavalent chromium removal from aqueous medium by activated carbon prepared from peanut shell: Adsorption kinetics, equilibrium and thermodynamic studies. *Chem. Eng. J.* **2012**, *184*, 238–247. [CrossRef]
27. Johari, K.; Saman, N.; Song, S.T.; Chin, C.S.; Kong, H.; Mat, H. Adsorption enhancement of elemental mercury by various surface modified coconut husk as eco-friendly low-cost adsorbents. *Int. Biodeterior. Biodegrad.* **2016**, *109*, 45–52. [CrossRef]
28. Sasmal, S.; Goud, V.V.; Mohanty, K. Characterization of biomasses available in the region of North-East India for production of biofuels. *Biomass Bioenergy* **2012**, *45*, 212–220. [CrossRef]
29. Jadhav, A.S.; Mohanraj, G.T. Synthesis and characterization of chemically activated carbon derived from *areca* nut shell. *Carbon Sci. Technol.* **2016**, *8*, 32–39.
30. Ranugadevi, N.; Anitha, G.; Lalitha, P. Kinetics of the removal of hexavalent chromium using a lowcost activated carbon adsorbent. *Adv. Appl. Sci. Res.* **2010**, *1*, 102–105.
31. Renugadevi, N.; Anitha, G.; Lalitha, P. Hexavalent chromium removal using a low-cost activated carbon adsorbent from *areca* catechu. *Indian J. Environ. Prot.* **2011**, *31*, 52–58.
32. Sundaram, M.M.; Sivakumar, S. Effective role of *areca* nut shell carbon and cashew nut shell carbon in the removal of congo red dye for the application towards effluent treatment. *Ind. J. Environ. Prot.* **2013**, *33*, 546–553.
33. Gopalswami, P.; Sivakumar, N.; Ponnuswamy, S.; Venkateswaren, V.; Kavitha, G. Adsorption of direct dye onto activated carbon prepared from *areca* nut pod—An agricultural waste. *J. Environ. Sci. Eng.* **2010**, *52*, 367–372. [PubMed]
34. Geetha, A.; Sivakumar, P.; Sujatha, M.; Palanisamy, P.N.; Somasundaram, V. Adsorption of acid blue from an aqueous solution onto activated *areca* nut shell carbon: Equilibrium, kinetic and thermodynamic studies. *Res. J. Chem. Environ.* **2009**, *13*, 52–58.
35. Guo, H.; Zhang, S.; Kou, Z.; Zhai, S.; Ma, W.; Yang, Y. Removal of cadmium(II) from aqueous solutions by chemically modified maize straw. *Carbohydr. Polym.* **2015**, *115*, 177–185. [CrossRef] [PubMed]

36. Aziz, A.; Elandaloussi, E.H.; Belhalfaoui, B.; Ouali, M.S.; De Ménorval, L.C. Efficiency of succinylated-olive stone biosorbent on the removal of cadmium ions from aqueous solutions. *Colloids Surf. B Biointerfaces* **2009**, *73*, 192–198. [CrossRef] [PubMed]
37. Clave, E.; François, J.; Billon, L.; Sèbe, G.; Jéso, B.D.; Guimon, M.F. Crude and modified corncobs as complexing agents for water decontamination. *J. Appl. Polym. Sci.* **2004**, *91*, 820–826. [CrossRef]
38. Gurgel, L.V.A.; Freitas, R.P.D.; Gil, L.F. Adsorption of Cu(II), Cd(II), and Pb(II) from aqueous single metal solutions by sugarcane bagasse and mercerized sugarcane bagasse chemically modified with succinic anhydride. *Carbohydr. Polym.* **2008**, *74*, 922–929. [CrossRef]
39. Thommes, M.; Kaneko, K.; Neimark, A.V.; Olivier, J.P.; Rodriguez-Reinoso, F.; Rouquerol, J.; Sing, K.S.W. Physisorption of gases, with special reference to the evaluation of surface area and pore size distribution (IUPAC Technical Report). *Pure Appl. Chem.* **2015**, *87*, 1051–1069. [CrossRef]
40. Yao, S.; Zhang, J.; Shen, D.; Xiao, R.; Gu, S.; Zhao, M.; Liang, J. Removal of Pb(II) from water by the activated carbon modified by nitric acid under microwave heating. *J. Colloid Interface Sci.* **2016**, *463*, 118–127. [CrossRef] [PubMed]
41. Lee, S.-M.; Lalhmunsiama; Choi, S.-I.; Tiwari, D. Manganese and iron oxide immobilized activated carbons precursor to dead biomasses in the remediation of cadmium-contaminated waters. *Environ. Sci. Pollut. Res.* **2013**, *20*, 7464–7477. [CrossRef] [PubMed]
42. Gurgel, L.V.A.; Júnior, O.K.; Gil, R.P.d.F.; Gil, L.F. Adsorption of Cu(II), Cd(II), and Pb(II) from aqueous single metal solutions by cellulose and mercerized cellulose chemically modified with succinic anhydride. *Bioresour. Technol.* **2008**, *99*, 3077–3083. [CrossRef] [PubMed]
43. Chadlia, A.; Mohamed, K.; Najah, L.; Farouk, M.M. Preparation and characterization of new succinic anhydride grafted Posidonia for the removal of organic and inorganic pollutants. *J. Hazard. Mater.* **2009**, *172*, 1579–1590. [CrossRef] [PubMed]
44. Tiwari, D.; Kim, W.; Kim, M.; Prasad, S.K.; Lee, S.-M. Organo-modified sericite in the remediation of phenol-contaminated waters. *Desalin. Water Treat.* **2015**, *53*, 446–451. [CrossRef]
45. Mudasir, M.; Karelius, K.; Aprilita, N.H.; Wahyuni, E.T. Adsorption of mercury(II) on dithizone-immobilized natural zeolite. *J. Environ. Chem. Eng.* **2016**, *4*, 1839–1849. [CrossRef]
46. Singanan, M. Biosorption of Hg(II) ions from synthetic wastewater using a novel biocarbon technology. *Environ. Eng. Res.* **2015**, *20*, 33–39. [CrossRef]
47. Liu, Q.-S.; Zheng, T.; Wang, P.; Jiang, J.-P.; Li, N. Adsorption isotherm, kinetic and mechanism studies of some substituted phenols on activated carbon fibers. *Chem. Eng. J.* **2010**, *157*, 348–356. [CrossRef]
48. Lalhmunsiama; Tiwari, D.; Lee, S.-M. Surface-functionalized activated sericite for the simultaneous removal of cadmium and phenol from aqueous solutions: Mechanistic insights. *Chem. Eng. J.* **2016**, *283*, 1414–1423.
49. Ho, Y.S.; Wase, D.A.J.; Forster, C.F. Kinetic studies of competitive heavy metal adsorption by sphagnum moss peat. *Environ. Technol.* **1996**, *17*, 71–77. [CrossRef]
50. Weber, W.J.; Morris, J.C. Kinetics of adsorption on carbon from solution. *J. Sanit. Eng. Div.* **1963**, *89*, 31–60.
51. Reddy, D.H.K.; Seshaiah, K.; Reddy, A.V.R.; Rao, M.M.; Wang, M.C. Biosorption of Pb^{2+} from aqueous solutions by Moringaoleifera bark: Equilibrium and kinetic studies. *J. Hazard. Mater.* **2010**, *174*, 831–838. [CrossRef] [PubMed]
52. Vasudevan, M.; Ajithkumar, P.S.; Singh, R.P.; Natarajan, N. Mass transfer kinetics using two-site interface model for removal of Cr(VI) from aqueous solution with cassava peel and rubber tree bark as adsorbents. *Environ. Eng. Res.* **2016**, *21*, 152–163. [CrossRef]
53. Hayes, K.F.; Papelis, C.; Leckie, J.O. Modeling ionic strength effects on anion adsorption at hydrous oxide/solution interfaces. *J. Colloid Interface Sci.* **1988**, *125*, 717–726. [CrossRef]
54. El-Bayaa, A.A.; Badawy, N.A.; Alkhalik, E.A. Effect of ionic strength on the adsorption of copper and chromium ions by vermiculite pure clay mineral. *J. Hazard. Mater.* **2009**, *170*, 1204–1209. [CrossRef] [PubMed]
55. Gokce, Y.; Aktas, Z. Nitric acid modification of activated carbon produced from waste tea and adsorption of methylene blue and phenol. *Appl. Surf. Sci.* **2014**, *313*, 352–359. [CrossRef]
56. Terzyk, A.P. Further insights into the role of carbon surface functionalities in the mechanism of phenol adsorption. *J. Colloid Interface Sci.* **2003**, *268*, 301–329. [CrossRef]
57. Zhang, D.; Huo, P.; Liu, W. Behavior of phenol adsorption on thermal modified activated carbon. *Chin. J. Chem. Eng.* **2016**, *24*, 446–452. [CrossRef]

58. Thomas, H.C. Heterogeneous Ion Exchange in a Flowing System. *J. Am. Chem. Soc.* **1944**, *66*, 1664–1666. [CrossRef]
59. Tiwari, D.; Laldanwngliana, C.; Choi, C.-H.; Lee, S.M. Manganese-modified natural sand in the remediation of aquatic environment contaminated with heavy metal toxic ions. *Chem. Eng. J.* **2011**, *171*, 958–966. [CrossRef]